



# Anti-CD79b/CD3 bispecific antibody combined with CAR19-T cells for B-cell lymphoma treatment

Wei-Wei Zheng<sup>1</sup> · Hang Zhou<sup>1,2</sup> · Ping Li<sup>3</sup> · Shi-Guang Ye<sup>3</sup> · Tuersunayi Abudureheman<sup>1</sup> · Li-Ting Yang<sup>1</sup> · Kai Qing<sup>4</sup> · Ai-Bin Liang<sup>3</sup> · Kai-Ming Chen<sup>1,5</sup> · Cai-Wen Duan<sup>1,2,5,6</sup>

Received: 28 January 2023 / Accepted: 11 August 2023 / Published online: 14 September 2023  
© The Author(s), under exclusive licence to Springer-Verlag GmbH Germany, part of Springer Nature 2023

## Abstract

CD19 CAR-T (chimeric antigen receptor-T) cell immunotherapy achieves a remission rate of approximately 70% in recurrent and refractory lymphoma treatment. However, the loss or reduction of CD19 antigen on the surface of lymphoma cells results in the escape of tumor cells from the immune killing of CD19 CAR-T cells (CAR19-T). Therefore, novel therapeutic strategies are urgently required. In this study, an anti-CD79b/CD3 bispecific antibody (BV28-OKT3) was constructed and combined with CAR19-T cells for B-cell lymphoma treatment. When the CD19 antigen was lost or reduced, BV28-OKT3 redirected CAR19-T cells to CD79b<sup>+</sup> CD19<sup>-</sup> lymphoma cells; therefore, BV28-OKT3 overcomes the escape of CD79b<sup>+</sup> CD19<sup>-</sup> lymphoma cells by the killing action of CAR19-T cells in vitro and in vivo. Furthermore, BV28-OKT3 triggered the antitumor function of CAR<sup>-</sup> T cells in the infusion product and boosted the antitumor immune response of bystander T cells, markedly improving the cytotoxicity of CAR19-T cells to lymphoma cells in vitro and in vivo. In addition, BV28-OKT3 elicited the cytotoxicity of donor-derived T cells toward lymphoma cells in vitro, which depended on the presence of tumor cells. Therefore, our findings provide a new clinical treatment strategy for recurrent and refractory B-cell lymphoma by combining CD79b/CD3 BsAb with CAR19-T cells.

**Keywords** CD79b/CD3 · Bispecific antibody · B-cell lymphoma · CAR19-T

## Abbreviations

ANOVA	One-way analysis of variance	CD3-BsAb	CD3-bispecific antibody
B-ALL	B-cell acute lymphoblastic leukemia	DLBCL	Diffuse large B-cell lymphoma
BCR	B-cell receptor	NHL	Non-Hodgkin lymphoma
BiTE	Bispecific T-cell engagers	PBMCs	Peripheral blood mononuclear cells
CAR-T	Chimeric antigen receptor T	scFv	Single-chain variable fragment
		TCR	T-cell receptor
		TILs	Tumor-infiltrating lymphocytes

Wei-Wei Zheng, Hang Zhou and Ping Li have contributed equally to this work.

✉ Ai-Bin Liang  
lab7182@tongji.edu.cn

✉ Kai-Ming Chen  
chenkaiming0001@126.com

✉ Cai-Wen Duan  
caiwenduan@sjtu.edu.cn

<sup>1</sup> Key Laboratory of Pediatric Hematology and Oncology Ministry of Health and Pediatric Translational Medicine Institute, Shanghai Children's Medical Center, Shanghai Jiao Tong University School of Medicine, Shanghai, China

<sup>2</sup> Department of Pathology, The Affiliated Hospital of Youjiang Medical University for Nationalities, Baise, China

<sup>3</sup> Department of Hematology, Tongji Hospital, Tongji University School of Medicine, Shanghai 200092, China

<sup>4</sup> State Key Laboratory of Medical Genomics, National Research Center for Translational Medicine at Shanghai, Shanghai Institute of Hematology, Ruijin Hospital Affiliated to Shanghai Jiao Tong University School of Medicine, Shanghai, China

<sup>5</sup> Fujian Branch of Shanghai Children's Medical Center Affiliated to Shanghai Jiaotong University School of Medicine and Fujian Children's Hospital, Fuzhou, China

<sup>6</sup> Key Laboratory of Technical Evaluation of Fertility Regulation for Non-Human Primate, National Health Commission, Fujian Maternity and Child Health Hospital, Fuzhou, China

## Introduction

Chimeric antigen receptor-T (CAR19-T) cells have been approved for treating B-cell malignancy by the FDA and have achieved a remission rate of approximately 70% in treating recurrent and refractory lymphoma [1–5]. CAR19-T cells have demonstrated exceptional success in the treatment of B-cell malignancy; however, many factors, such as the lack of CAR-T cell persistence [6], loss or modulation of the target antigen [7], and the tumor immunosuppressive microenvironment in tumors, preclude long-term remission following CAR19-T therapy [8]. In clinical practice, CD19-negative relapse is a major problem in patients with hematologic malignancies who receive CAR19-T cell infusion [9, 10]. Among patients with B-cell acute lymphoblastic leukemia (B-ALL), approximately 20–30% of relapses are attributed to the loss of CD19 on the tumor cell surface. Autopsy sample testing revealed that the CD19 antigen was negatively expressed in approximately 30% of the patients with recurrent B-cell NHL [11]. Previous studies have suggested that the loss or reduction of the CD19 epitope on the surface of tumor cells is caused by alternative splicing or obstruction of CD19 transport to the cell membrane [12]. In addition, CAR19-T treatment results in reversible antigen loss on the tumor cell surface through trogocytosis [13], reducing CD19 density and enabling the escape of tumor cells from CAR19-T surveillance. Therefore, identifying new tumor targets and developing novel strategies are imperative to overcome resistance to CAR19-T therapy.

CD79b is a B-cell surface antigen and a component of the B-cell receptor (BCR). Normally, CD79b specifically combines with CD79a to form a BCR complex only during the late stage of B cell differentiation [14]. Clinical analysis of patient samples revealed that the CD79b protein was distinctively expressed in over 90% of B-cell NHL cases [15, 16], suggesting that CD79b is a potential target for the clinical treatment of lymphoma. Polatuzumab vedotin, an antibody–drug conjugate, was developed to target the CD79b antigen and approved by the FDA in 2019. In the clinical setting, polatuzumab vedotin combined with bendamustine and rituximab has been used to treat relapsed and refractory DLBCL in patients who have undergone at least two rounds of treatment [17]. A recent study revealed that an anti-CD79b/CD3 bispecific antibody is a potential treatment for B-cell malignancies [18]. However, anti-CD79b/CD3 bispecific antibodies with a bispecific T-cell engagers (BiTE) structure combined with CAR-T cells have not yet been reported for lymphoma treatment.

Treatment with CD3-bispecific antibody (CD3-BsAb) is an alternative strategy for mobilizing and boosting T cells [19]. CD3-BsAbs have two antigen-binding domains, one

of which binds T cells, and the other binds distinct antigens on the surface of tumor cells. CD3-BsAbs link the tumor cell antigen and the CD3 $\epsilon$  unit of the T-cell receptor (TCR) via antibody-binding regions, thereby bypassing major histocompatibility complex restriction and leading to the activation of cytotoxic T cells and subsequent tumor lysis [20]. Blinatumomab, a CD19 and CD3 bispecific antibody, has been approved by the FDA for refractory B-ALL treatment and provides long-term clinical response [21]. Given the potential of CD79b as a target for antibody-based therapeutics, we developed an anti-CD79b/CD3 bispecific antibody combined with CAR19-T cells to treat B-cell lymphoma and overcome the relapse frequently associated with the loss of the CD19 antigen.

## Materials and methods

### Cell lines and primary cells

Cell lines: Ramos was provided by Tongji Hospital (Shanghai, China). SU-DHL-4 and DB were purchased from Procell Life Science & Technology Co., Ltd., (Wuhan, China) and Nalm6 was purchased from ATCC. Cells were cultured in RPMI-1640 medium supplemented with 10% FBS (Gibco, USA), penicillin, and streptomycin (NCM biotech, Suzhou, China). We purchased 293 T cells from the National Collection of Authenticated Cell Cultures and cultured them in HEK293 MaxD medium with 3% MaxFA6 and 0.3% MaxFB (MediumBank, Shanghai, China).

Peripheral blood mononuclear cells (PBMCs): Blood from healthy donors was collected into tubes containing ethylenediaminetetraacetic acid. PBMCs were collected via density gradient centrifugation using human PBMC isolation buffer (Dakewe Biotech, Shenzhen, China) and then cultured in CTST<sup>TM</sup> AIM V<sup>TM</sup> SFM medium (Gibco, USA) with 4% FBS and 300 Unit/mL IL2 (SL pharm, Beijing, China). PBMCs were continuously cultured for 5–12 days after activation for 48 h with anti-human CD3 and anti-human CD28 antibodies (5  $\mu$ g/mL, Sino Biological Inc, Beijing, China).

Primary lymphoma cells: Pleural fluid or ascites from patients with DLBCL were obtained from Tongji Hospital and centrifuged at 1500 rpm for 5 min. After counting the cell number, the cells were cultured in a complete 1640 medium, and the remaining cells were preserved in CELL-SAVING<sup>TM</sup> (NCM, Suzhou, China).

## Protein production

BV28-OKT3, OKT3-scFv-IgG1 Fc, and BV28-scFv-IgG1 Fc antibodies were individually expressed using the pSB-BV28-OKT3-cMyc-His, pSB-OKT3-scfv-IgG1 Fc, and pSB-BV28-scfv-IgG1 Fc plasmids, respectively.

Using the Lipofectamine 3000 transfection reagent (Life Technologies, USA), 293 T cells were transfected with the target protein expression vector, and stable expression was achieved by selection with 2 µg/mL puromycin. The proteins were purified from the culture supernatant using gravity chromatography columns filled with Ni-IDA. The culture supernatant of 293 T cells was centrifuged at 3000 rpm for 5 min. After centrifugation, the supernatant was loaded onto a column. Finally, the column containing the bound protein was washed with 20 and 40 mM imidazole and eluted with 200 and 500 mM imidazole. Amicon® Ultra-4 10 K centrifugal filter devices (Merk, USA) were used to concentrate and dialyze the proteins in PBS thrice.

The amino acid sequences of the three antibodies are presented in the supplementary text.

## Generation of CAR-T cells

Tongji Hospital (Shanghai, China) provided plasmids containing CD19-CAR, whereas those containing CD123-CAR were preserved in the laboratory. The two plasmids were individually cotransfected with psPAX2 (Addgene number: #12,260) and pMD2.G (Addgene number: #12,259) into HEK293T cells. The viral particles were collected after 48 and 72 h.

PBMCs were collected as previously described. T cells were transduced with the indicated viruses and 10 µg/mL of polybrene after 48 h of stimulation with anti-human CD3 and CD28 antibodies. The ratio of CAR-positive cells was determined by flow cytometry 48 h after transduction.

## Xenograft models

Severely immunocompromised *Prkdc<sup>scid</sup>Il2rg<sup>em1</sup>*/Smoc (NSG) mice (male, 6–8 weeks old) were purchased from the Shanghai Model Organisms Center. Mice were subcutaneously inoculated with  $1 \times 10^7$  SU-DHL-4 or SU-DHL-4 CD19 KO cells in 75 µL of PBS and an equal volume of Matrigel (356,234, BD, USA) or with  $5 \times 10^6$  SU-DHL-1 cells in 100 µL of PBS. When the tumor volume reached approximately 100 mm<sup>3</sup>,  $4 \times 10^6$  CD19 CAR-T with 30–40% CAR-positive or  $1 \times 10^7$  T cells were incubated with 1 µg/mL BV28-OKT3 for 2 h in vitro and then infused via tail

injection. On the second day, 50 µL (10 µg/mL) of BV28-OKT3 or PBS was injected intratumorally once daily for 6 days. The tumor volume and mouse weight were measured daily or on alternate days. At the end of the experiment, the mice were euthanized, and the tumors were harvested and photographed.

The tumor volume (V) was calculated as  $V = L \times W^2/2$ .

One-way analysis of variance (ANOVA) was used to analyze the tumor volume and body weight at the end of the experiment.

## Statistical analyses

Two-tailed unpaired t-tests were used to compare two groups. One-way ANOVA was used to compare three or more groups in a single condition. All values in the study were expressed as the mean ± standard deviation. Statistical analyses were performed using Graph Prism 9. Differences with  $P < 0.05$  (\*),  $P < 0.01$  (\*\*),  $P < 0.001$  (\*\*\*), and \*\*\*\*  $P < 0.0001$  (\*\*\*\*) were considered significant.

## Results

### CD79b is an appropriate target for lymphoma treatment

The CD19 antigen expressed on the surface of tumor cells is the most promising target for CAR-T treatment. Clinically, the loss or downregulation of CD19 leads to the recurrence of B-cell lymphoma after CAR19-T cell treatment. The expression of B-cell antigens on the surface of tumor cells in patients with DLBCL was detected to identify other surface antigens of B-cell lymphoma as potential targets for CAR19-T cell therapy. CD79b was highly expressed in all the patients, whereas CD19 was absent or expressed at low levels (Figure S1A). In addition, CAR19-T treatment results in the loss of CD19, but not CD79b, in relapsed B-cell lymphoma (Figure S1B). Therefore, CD79b was used as alternative target to construct a CD3-BsAb to overcome CD19-negative relapse during CAR-T cell treatment.

### Production of anti-CD79b/CD3 bispecific antibody (BV28-OKT3)

BV28-OKT3 was designed as a BiTE structure [22, 23] that fuses a second N-terminal single-chain variable fragment (scFv) domain derived from a CD79b-specific antibody (BV28) (patent CN104540526A) with a C-terminal scFv domain derived from a CD3-specific antibody (OKT3). BV28 and OKT3 bispecific antibody was connected via a

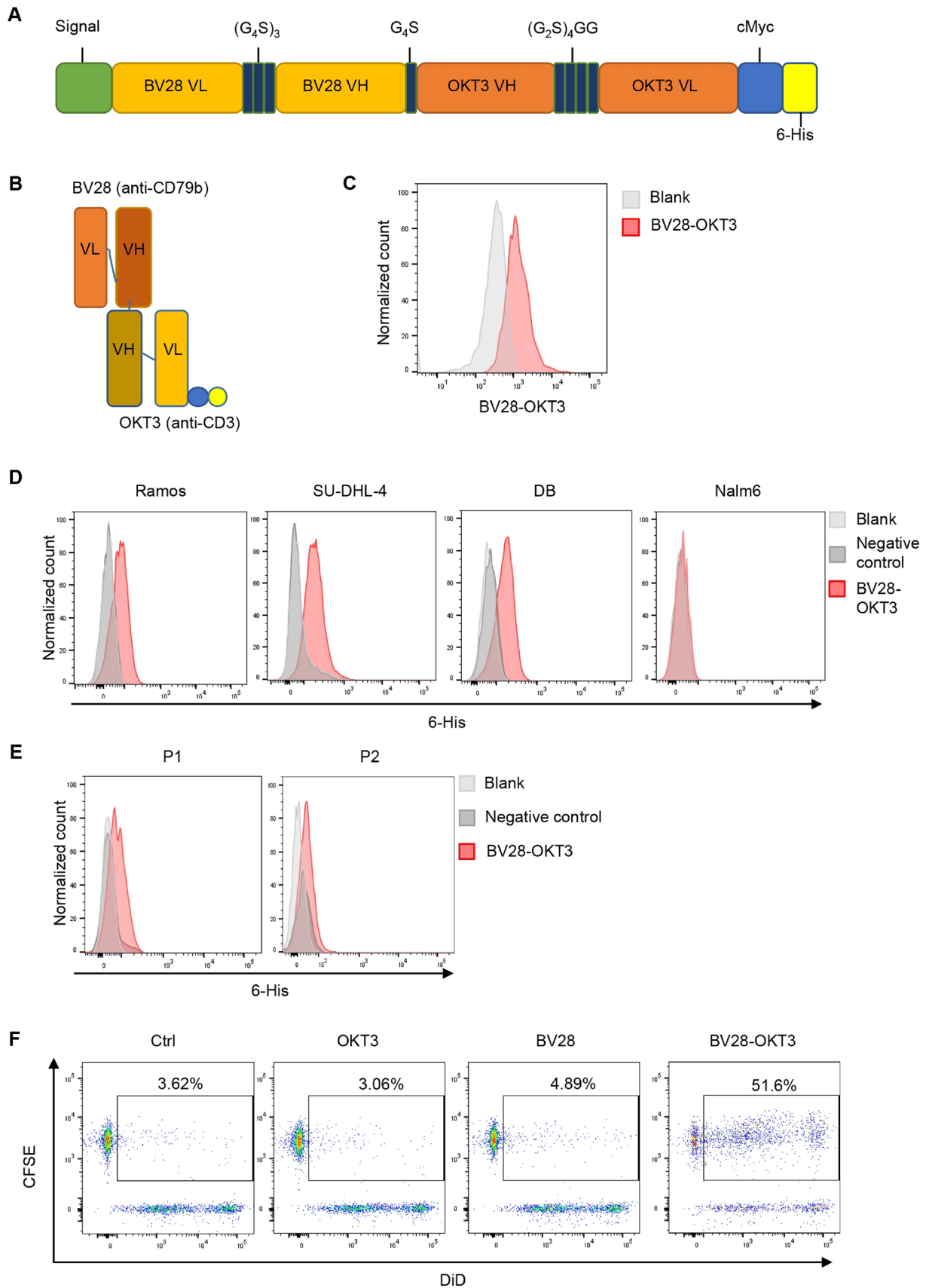


**Fig. 1** Production of CD79b/CD3 bispecific antibody (BV28-OKT3) **A** Vector construction of BV28-OKT3; (G<sub>4</sub>S)<sub>3</sub>, G<sub>4</sub>S, and (G<sub>2</sub>S)<sub>4</sub>GG are linkers; c-Myc and 6 His tag are tags. VL: variable region of the light chain. VH: variable region of the heavy chain. **B** Protein structure of BV28-OKT3. Blue: c-Myc tag. Yellow: 6 His tag; **C–E** Flow cytometry analysis of the binding capability of BV28-OKT3 with T cells **C**, Cell lines: Ramos, DB, SU-DHL-4, and Nalm6 **D**, Primary lymphoma cells isolated from patients **E**, Samples without staining were indicated as blank and negative control were cells only incubated with anti-6 His tag antibody; **F** T and SU-DHL-4 cells were co-cultured for 2 h with or without indicated antibodies. SU-DHL-4 cells were stained with DiD (APC), and T cells were stained with CFSE (FITC). Double-positive cells were assessed using FCM

G<sub>4</sub>S linker to provide flexibility to the two scFv domains. In addition, c-myc and 6-His tags were added to purify and detect antibodies (Fig. 1A–B). The BV28-OKT3 fragment was cloned into the pSB vector, and the antibody was expressed in HEK293T cells and purified using Ni-IDA Sefinose resin. The purity and identity of BV28-OKT3, with an expected molecular weight of approximately 55 kDa, were determined using SDS-PAGE (Figure S2A). The expression of BV28-OKT3 was also determined using an anti-human c-Myc antibody (Figure S2B). OKT3-scFv-IgG1 Fc and BV28-scFv-IgG1 Fc antibodies were constructed as control proteins and referred to as OKT3 and BV28, respectively (Figures S3A–B).

## BV28-OKT3 modulates the cytotoxicity of T cells

To verify whether BV28-OKT3 could bind to the CD79b and CD3 antigens, we first evaluated the combination of BV28-OKT3 with the CD3 antigen. PBMCs were isolated from healthy donors and stimulated with anti-human CD3 and anti-human CD28 antibodies for 48 h, with the purity of T cells over 95% (Figure S4A). Flow cytometry analysis demonstrated that BV28-OKT3 strongly bound to the CD3 antigen on the T cell surface (Fig. 1C). We then evaluated the combination of BV28-OKT3 and CD79b antigens in lymphoma cell lines such as Ramos, SU-DHL-4, and DB, which highly express CD79b and CD19 (Figure S4B). Flow cytometry analysis revealed that BV28-OKT3 was strongly associated with Ramos, SU-DHL-4, and DB cells but not with Nalm6, a B-ALL cell line that positively expresses CD19 and does not express CD79b (Fig. 1D; Figure S4B). Moreover, the binding efficiency of BV28-OKT3 to CD79b was confirmed in samples from patients with lymphoma (Fig. 1E). The ability of OKT3 and BV28 to bind to their target proteins was also verified (Figures S4C–D).

To further determine whether BV28-OKT3 could simultaneously bind to lymphoma cells and T cells, SU-DHL-4 and T cells were stained with DiD and CFSE, respectively, and co-cultured with BV28-OKT3, OKT3, or BV28. If

BV28-OKT3 facilitates the combination of lymphoma and T cells, then a population of DiD and CFSE double-positive cells can be detected by flow cytometry. The proportion of double-positive cells was approximately 50% in the presence of BV28-OKT3, whereas only 4% of double-positive cells were detected in the presence of BV28 or OKT3 antibodies (Fig. 1F). These results suggest that BV28-OKT3 successfully connects T cells to lymphoma cells.

The cytotoxicity of T cells mediated by BV28-OKT3 was proved. T cells were isolated from healthy donors and incubated with Ramos and SU-DHL-4 cells in the presence of BV28-OKT3, BV28, or OKT3 for 24 h. The cytotoxicity of T cells to lymphoma cells was measured by LDH detection kit (Fig. 2A, B). The results revealed that BV28-OKT3 prompted donor-derived T cells to kill SU-DHL-4 and Ramos cells, with a specific lysis ratio of 45% to 70%. However, treatment with a high concentration of BV28-OKT3 (10 µg/mL) alone did not affect the viability of the lymphoma cells (Figure S4E). Moreover, the anti-CD3 antibody OKT3 slightly enhanced the killing capability of T cells toward SU-DHL-4, indicating that OKT3 mildly activated T cells. Furthermore, the T cell-mediated lysis of lymphoma cells depended on the dose of BV28-OKT3 and the number of T cells (Fig. 2C, D). In addition, BV28-OKT3 did not stimulate T-cells against Nalm6, which does not express CD79b, suggesting that BV28-OKT3 possesses specificity and safety in vitro and in vivo.

Donor-derived T-cells were injected into mice with lymphoma treated with or without BV28-OKT3 (Fig. 3A). BV28-OKT3 markedly improved the antitumor activity of donor-derived T-cells and compromised tumor growth in vivo (Fig. 3B, C, D). In contrast, donor-derived T-cell treatment or BV28-OKT3 alone did not affect the growth of tumor neoplasms compared with the control (Fig. 3E, F). In addition, BV28-OKT3 resulted in the local expansion of T cells within the tumor tissues (Fig. 3G), indicating that BV28-OKT3 enhanced the cytotoxic killing of donor-derived T cells by recruiting these cells into the tumor. Therefore, the function of this bispecific antibody in modulating T-cell cytotoxicity was verified.

## BV28-OKT3 overcomes CD19 antigen escape of tumor cells from the killing of CAR19-T cells in vitro and in vivo

Loss or low expression of the CD19 antigen mainly contributes to the escape of tumor cells from CAR19-T therapy [24]. To determine whether BV28-OKT3 can redirect CD79b<sup>+</sup> CD19<sup>-</sup> lymphoma cells to CAR19-T cells, a second-generation CAR19-T cell was established using 4-1BB as a co-stimulatory molecule. CAR19 comprises an extracellular FMC63 scFv, a transmembrane region, and a

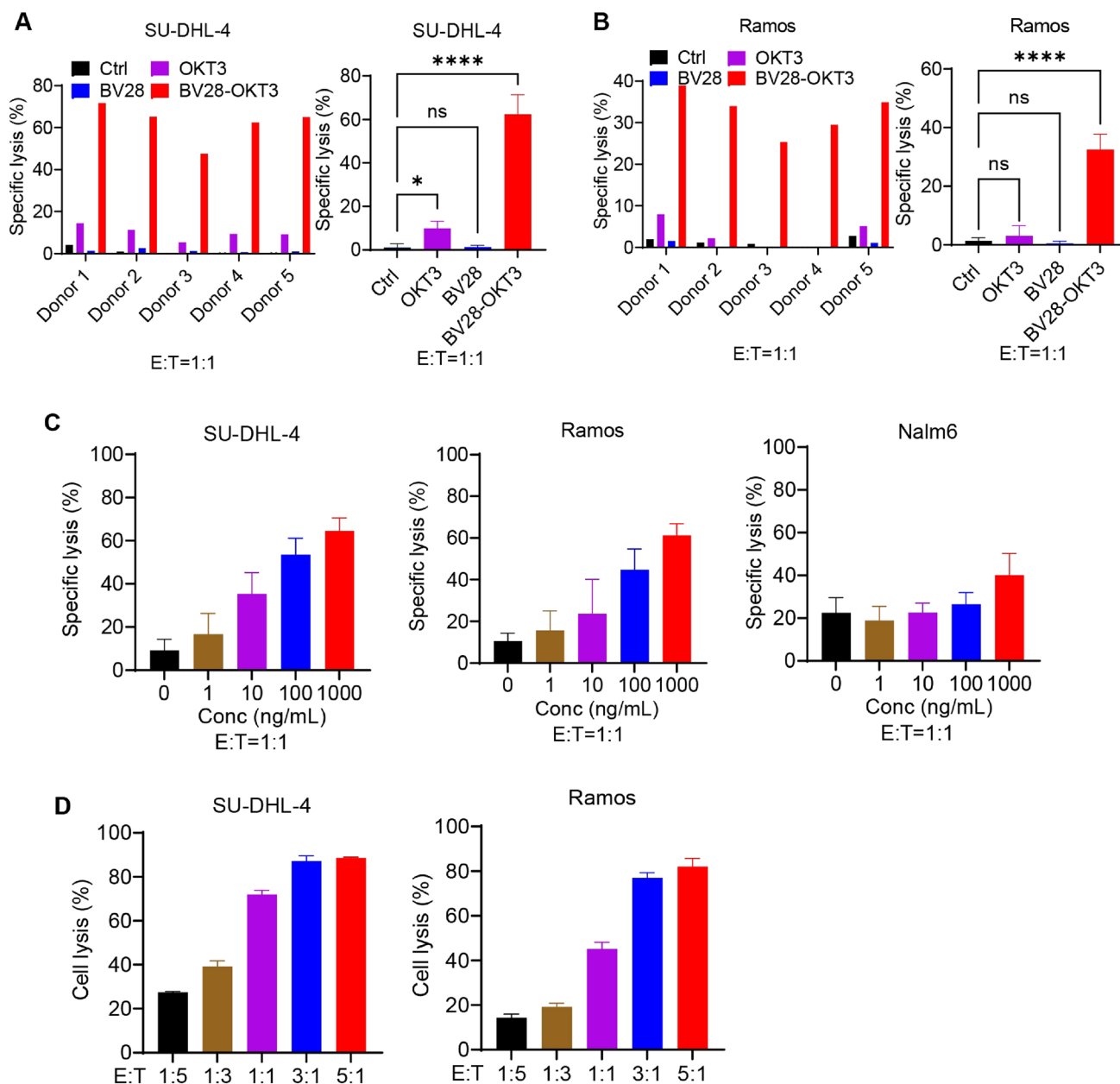


**Fig. 2** BV28-OKT3 induces the cytotoxicity of T cells to lymphoma cells in vitro **A**, **B** Cytotoxicity of T cells from different donors in SU-DHL-4 **A** and Ramos cells **B** T cells and lymphoma cells (E:T=1:1) were incubated with 1  $\mu$ g/mL antibodies for 24 h, and the specific lysis ratio of the cells was detected using an LDH detection kit; **C** Lymphoma cell lines were co-cultured with T cells at an E:T

ratio of 1:1 in the presence of the indicated concentrations of BV28-OKT3 for 24 h. The specific lysis ratio was determined using an LDH detection kit; **D** CFSE-labeled lymphoma cell lines were co-cultured with T cells in the presence of 50 ng/mL BV28-OKT3 for 24 h at the indicated E:T ratios. The percentage of lysed cells was quantified using FCM

cytoplasmic region of human 4-1BB and CD3 $\zeta$  (Fig. 4A). T cells were isolated from the PBMCs of healthy donors, stimulated for 48 h, and then infected with CAR19 lentivirus (Fig. 4B). CAR expression was detected using an anti-FMC63 antibody, and the percentage of CAR-positive cells was approximately 80% (Fig. 4C). Flow cytometry and cell killing analyses indicated that CAR-T cells were activated

by Nalm6, which expressed CD19, but not by Jurkat cells, which did not express CD19 (Figure S5).

CD19-negative (CD19-KO) SU-DHL-4 cells were established using CRISPR/CAS9. The expression of CD19 was reduced, whereas that of CD79b remained unchanged (Figure S6A). These cells were co-cultured with CAR19-T cells in the presence of BV28-OKT3, OKT3, or BV28. The results revealed that BV28-OKT3 promoted the reconnection

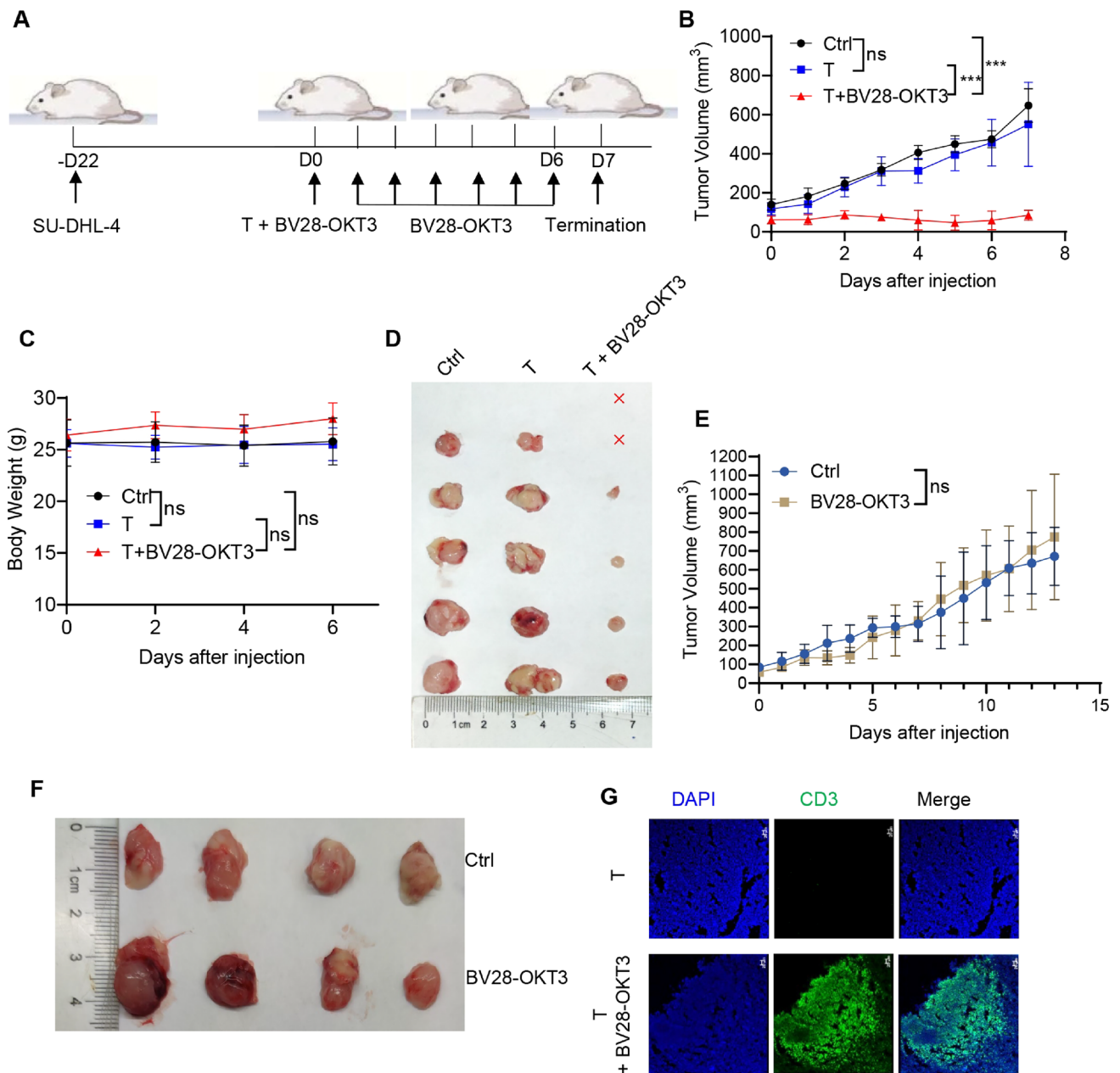


**Fig. 3** BV28-OKT3 induces the cytotoxicity of T cells to lymphoma cells in vivo **A** Schematic representation depicts the xenograft mouse model. NSG mice were subcutaneously injected with  $1 \times 10^7$  SU-DHL-4 cells. When tumors reached a volume of approximately  $100 \text{ mm}^3$ , mice were randomized into three groups and received different treatments: Control group ( $n=5$ ), T group ( $n=5$ ), T+BV28-OKT3 group ( $n=6$ ); **B** Tumor growth curves of all mice are shown (means  $\pm$  SD). One-way ANOVA was used for analysis at D7. \*,  $P < 0.05$ ; \*\*,  $P < 0.01$ ; \*\*\*,  $P < 0.001$ ; **C** Weight change curves of all mice (means  $\pm$  SD); One-way ANOVA was used at D6; **D** Images of the tumors harvested from the mice at the end of the experiment, where red x indicates the disappearance of the tumor; **E–F** NSG mice

were subcutaneously injected with  $1 \times 10^7$  SU-DHL-4 cells. When tumors reached a volume of  $100 \text{ mm}^3$ , mice were randomized into the following treatment groups: Control group ( $n=4$ ), mice were injected with PBS intravenously at D0, and  $50 \mu\text{L}$  PBS intratumorally every day at D1–D6; BV28-OKT3 group ( $n=4$ ), mice were injected with  $1 \mu\text{g}/\text{mL}$  BV28-OKT3 D0, and  $50 \mu\text{L}$   $10 \mu\text{g}/\text{mL}$  BV28-OKT3 intratumorally every day at D1–D6; Tumor growth curves of all mice are shown (means  $\pm$  SD). One-way ANOVA was used for analysis on D13 **E**; Images of the tumors harvested from the mice at the end of the experiment **F**; **G** Representative tumor images obtained by confocal microscopy were shown. Blue indicates Dapi, and green indicates CD3

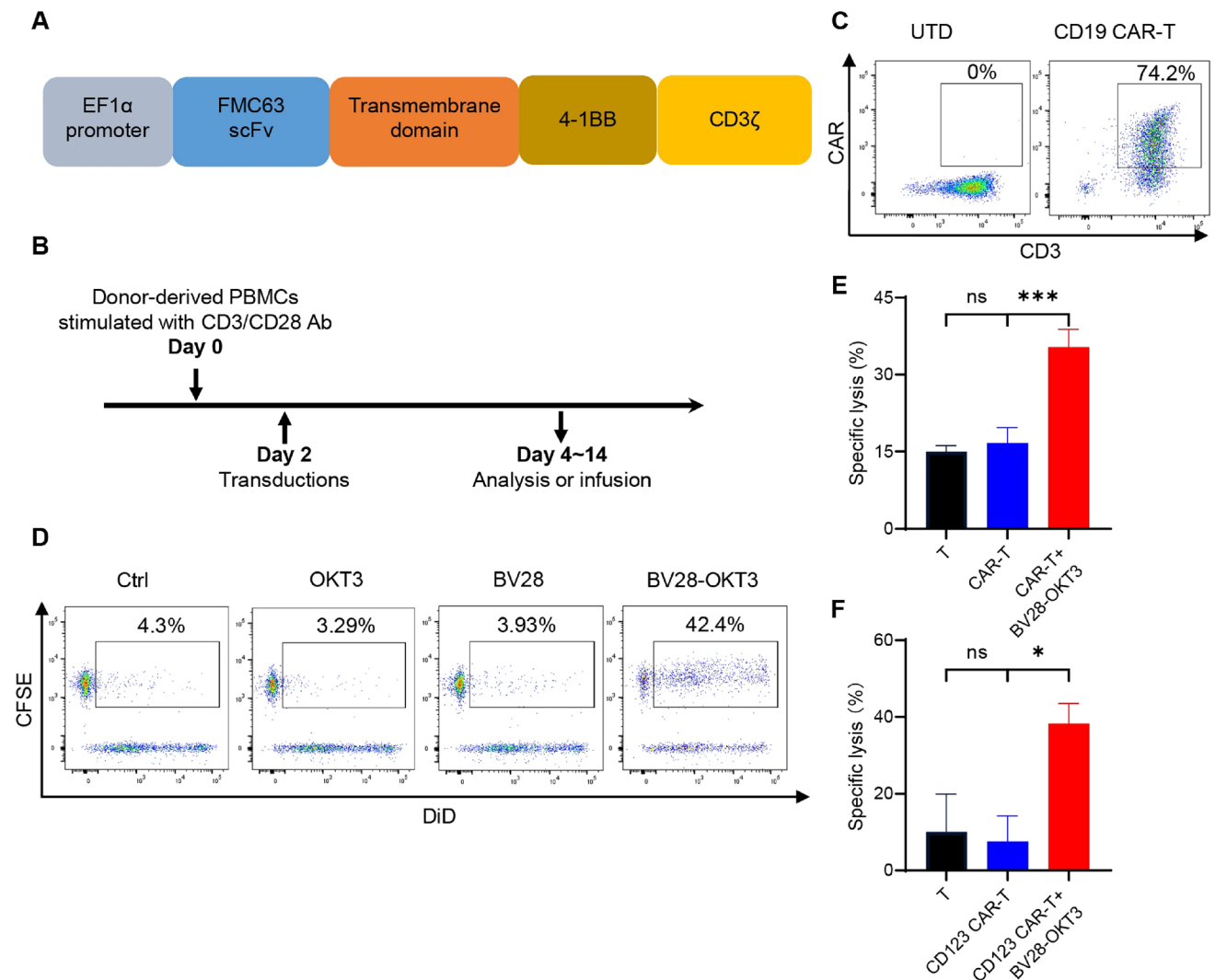


**Fig. 4** BV28-OKT3 overcomes CD19 antigen escape of tumor cells from killing of CAR19-T cells in vitro **A** Structure of CAR19; **B** Schema of generation of CAR19-T cells; **C** The expression levels of CAR and CD3 were analyzed by flow cytometry. UTD indicates untransduced T cells; **D** CAR-T and CD19-KO SU-DHL-4 cells were co-cultured for 2 h with or without indicated antibodies. CD19-KO SU-DHL-4 cells were stained with DiD (APC), and CAR-T cells were stained with CFSE (FITC). Double-positive cells were assessed

of CD19-KO SU-DHL-4 cells with CAR19-T cells compared with OKT3 or BV28 cells (Fig. 4D). The results of the cell cytotoxicity analysis demonstrated that BV28-OKT3 facilitated the killing effect of CAR19-T cells on CD19-KO SU-DHL-4 cells (Fig. 4E), indicating that BV28-OKT3 redirected CAR19-T cells to CD79b-positive tumor cells with CD19 antigen loss and mediated the killing ability of CAR19-T cells.

CD123 CAR-T cells (CAR123-T) were also generated to treat Ramos cells that expressed CD79b, but not the CD123 antigen, to further mimic the loss or downregulation of the CD19 antigen after CAR19-T treatment. The

using FCM; E T cells or CAR19-T cells were co-cultured with CFSE-labeled CD19-KO SU-DHL-4 cells at E:T as 1:1 for 24 h with or without 50 ng/mL BV28-OKT3. The percentage of specific cell lysis ratio was quantitated by FCM; **F** T cells or CAR123-T cells were co-cultured with Ramos cells at E:T as 1:1 for 24 h with or without 50 ng/mL BV28-OKT3. LDH detection kit was used to analyze the specific lysis ratio of Ramos

structure of CAR123 is similar to that of CAR19 and comprises an extracellular scFv anti-CD123 antibody, a transmembrane region, and a cytoplasmic region of human 4-1BB, CD3ζ, and GFP moieties (Figure S6B). CAR expression was determined by measuring GFP expression levels (Figure S6C). The cytotoxicity analysis confirmed that BV28-OKT3 dramatically enhanced the killing capability of CAR123-T in Ramos cells (Fig. 4F). These findings thus suggest that BV28-OKT3 contributes to the cytotoxicity of CAR123-T cells by combining CAR-T cells with CD79b-positive tumor cells despite the absence of the CD123 antigen on the surface of tumor cells.



To evaluate whether BV28-OKT3 cells overcome the escape of immunotherapy due to the loss of CD19 antigen *in vivo*, CD19-KO SU-DHL-4 cells were subcutaneously injected into NOD-*Prkdc*<sup>scid</sup>*Il2rg*<sup>em1</sup>/Smoc (NSG) mice to establish a tumor xenograft mouse model with CD19 antigen loss (Fig. 5A). After incubation with BV28-OKT3 for 2 h *in vitro*, CAR19-T cells were injected via the tail vein, and BV28-OKT3 was intratumorally administered to circumvent the barriers of the tumor microenvironment from day 1. The results revealed that treatment with BV28-OKT3 or CAR19-T alone did not affect the growth of tumor neoplasms, whereas BV28-OKT3 notably reactivated the antitumor function of CAR19-T cells and retarded tumor growth *in vivo* (Fig. 5B–F). Furthermore, BV28-OKT3 treatment resulted in an increase in T cells within tumor tissues (Fig. 5G). CAR-T cells from another donor also suggested that BV28-OKT3 recruited CAR19-T cells into the tumor and modulated the cytotoxic killing of CAR19-T cells on lymphoma cells with CD19 antigen loss *in vivo*, but not OKT3 (Figure S7). In addition, BV28-OKT3 did not mediate CAR19-T cells to kill SU-DHL-1 *in vivo*, which do not express CD79b (Figure S8).

### BV28-OKT3 promotes antitumor effects of bystander T cells *in vitro* and *in vivo*

Bystander T cells do not recognize tumor-specific antigens in tumor tissues [25, 26]. The proportion of CAR-positive (CAR<sup>+</sup>) T cells is between 30 and 50% during CAR19-T cell production *in vitro* due to the heterogeneity of T cells in patients [27], indicating that CAR-negative (CAR<sup>-</sup>) T cells (a type of bystander T cell) occupy 50–70% of infused CAR-T cells. Thus, it remains unknown whether BV28-OKT3 activates CAR<sup>-</sup> T cells. To evaluate this, the multiplicity of lentiviral infection was decreased, and the ratio of CAR<sup>+</sup> cells was adjusted to approximately 50% (Figure S9A). Lymphoma cells were then co-cultured with CAR19-T cells in the presence of BV28-OKT3 cells, and the cell lysis ratio of the lymphoma cells was determined. BV28-OKT3 and CAR19-T cells exhibited synergistic cytotoxicity toward lymphoma cells, including Ramos, SU-DHL-4, and DB (Fig. 6A). The activation status of CAR<sup>-</sup> T cells after co-culturing with tumor cells was determined to gain further insight into whether the cytotoxicity of CAR-T cells enhanced by BV28-OKT3 partially contributed to the activity of CAR<sup>-</sup> T cells. BV28-OKT3 remarkably increased CD25 and CD69 expression in CAR<sup>-</sup> T cells and promoted the secretion of IL2, IFN $\gamma$ , and TNF $\alpha$  of CAR<sup>-</sup> T cells (Fig. 6B–E; Figure S10). In addition, BV28-OKT3 did not promote the exhaustion of CAR<sup>+</sup> T cells by staining the T-cell exhausted marker, Tim3 (Figure S11).

Next, we investigated whether BV28-OKT3 could improve the antitumor activity of CAR-T cells against CD19<sup>+</sup> lymphoma cells *in vivo* (Fig. 7A). CAR19-T cell treatment alone suppressed the growth of tumor neoplasms compared with the control. BV28-OKT3 enhanced the antitumor function of CAR19-T cells and alleviated tumor growth (Fig. 7B–D). Further, BV28-OKT3 increased the number of CD8<sup>+</sup> T cells within tumor tissues (Fig. 7E). These findings were confirmed with CAR-T cells from another donor (Figure S12). These findings indicated that BV28-OKT3 promotes the antitumor effects of bystander CAR<sup>-</sup> T cells *in vitro* and *in vivo*.

### BV28-OKT3-mediated T cell activation depends on the presence of tumor cells

Whether BV28-OKT3-mediated T cell activation depends on the presence of CD79b-positive lymphoma cells was further investigated. BV28-OKT3 induced T cell activation in the presence of CD79b<sup>+</sup> SU-DHL-4 cells (Figure S13). In contrast, neither CD79b<sup>+</sup> SU-DHL-4 cells nor the BV28-OKT3 antibody alone activated T cells. These data indicate that T cell activation mediated by BV28-OKT3 relies on CD79b-positive tumor cells, which may introduce a few toxic side effects *in vivo*. BV28-OKT3 did not induce the development of CAR19-T cells in a progressively worsening disease characterized by weight loss (Fig. 7C). In addition, HE staining of the heart, liver, and kidneys demonstrated that BV28-OKT3 did not influence CAR19-T cells to induce organ lesions (Figure S14). These results reveal that BV28-OKT3 promotes T cell activation in combination with the CD79b antigen.

## Discussion

The threshold density of the targeted antigen is vital in the modulation of CAR-T cells and tumor synapses. Hence, the loss or downregulation of the CD19 antigen epitope on the lymphoma surface contributes to the immune escape of CAR19-T cells. In addition to CAR19-T, CAR20-T, CAR22-T, CAR19, and CAR20, bispecific CAR-T cells have also been used in clinical trials to treat refractory/relapsed B-cell malignancies [11, 28]. Nevertheless, CD20- and CD22-negative relapses occur during CAR T-cell treatment [29, 30]. However, CD79b antigen loss has not been reported after clinical administration of polatuzumab vedotin, indicating that CD79b is a potential therapeutic target for lymphoma treatment [31, 32]. A recent study revealed that anti-CD79b CAR-T cells could treat and prevent CD19 antigen escape from B-cell lymphoma [33]. Here, BV28-OKT3, which

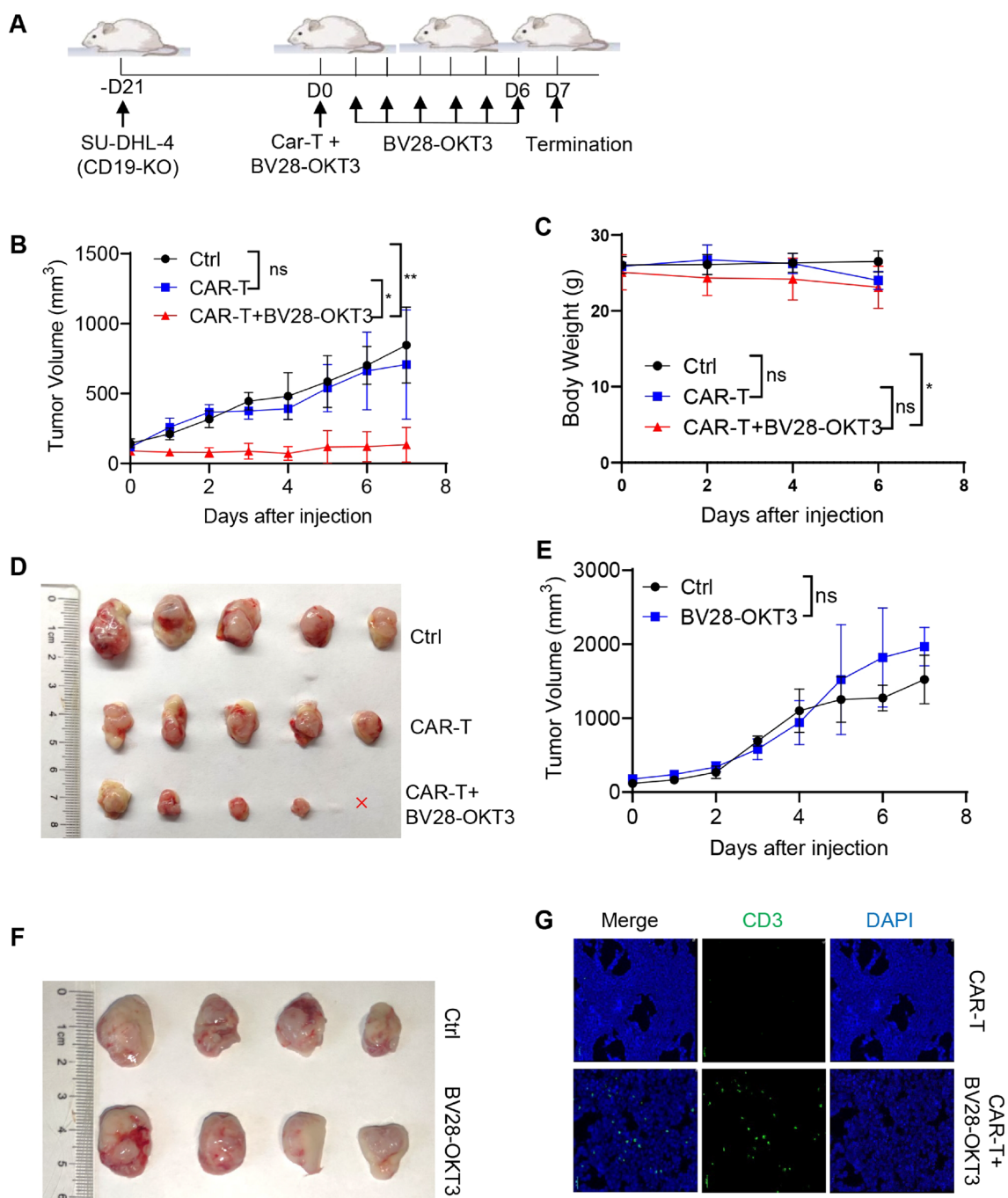


**Fig. 5** BV28-OKT3 combined with CAR-T cells retard the progression of CD19-negative tumor cells in vivo **A** Schematic representation depicts the xenograft mouse model. NSG mice were subcutaneously injected with  $1 \times 10^7$  CD19-KO SU-DHL-4 cells. When tumors reached a volume of approximately  $100 \text{ mm}^3$ , mice were randomized into three groups and received different treatments, five mice per group; **B** Tumor growth curves of all mice are illustrated (means  $\pm$  SD). One-way ANOVA was used for analysis at D7. \*,  $P < 0.05$ ; \*\*,  $P < 0.01$ ; **C** Weight change curves of all mice are presented (means  $\pm$  SD); One-way ANOVA was used for analysis at D6. \*,  $P < 0.05$ ; **D** Images of the tumors harvested from the mice at the end of the experiment, where red x denotes the dis-

appearance of tumor; **E–F** NSG mice were subcutaneously injected with  $1 \times 10^7$  CD19-KO SU-DHL-4 cells. When tumors reached a volume of approximately  $100 \text{ mm}^3$ , mice were randomized into the following treatment groups: Control group ( $n = 4$ ), mice were injected with PBS intravenously at D0, and  $50 \mu\text{L}$  PBS intratumorally daily at D1–D6; BV28-OKT3 group ( $n = 4$ ), mice were injected with  $1 \mu\text{g}/\text{mL}$  BV28-OKT3 D0, and  $50 \mu\text{L}$   $10 \mu\text{g}/\text{mL}$  BV28-OKT3 intratumorally daily from D1 to D6; Tumor growth curves of all mice are shown (means  $\pm$  SD). One-way ANOVA was used for analysis on D7 **E**; Images of the tumors harvested from the mice at the end of the experiment **F**; **G** Representative tumor images obtained by confocal microscopy are shown. Blue indicates Dapi, and green indicates CD3

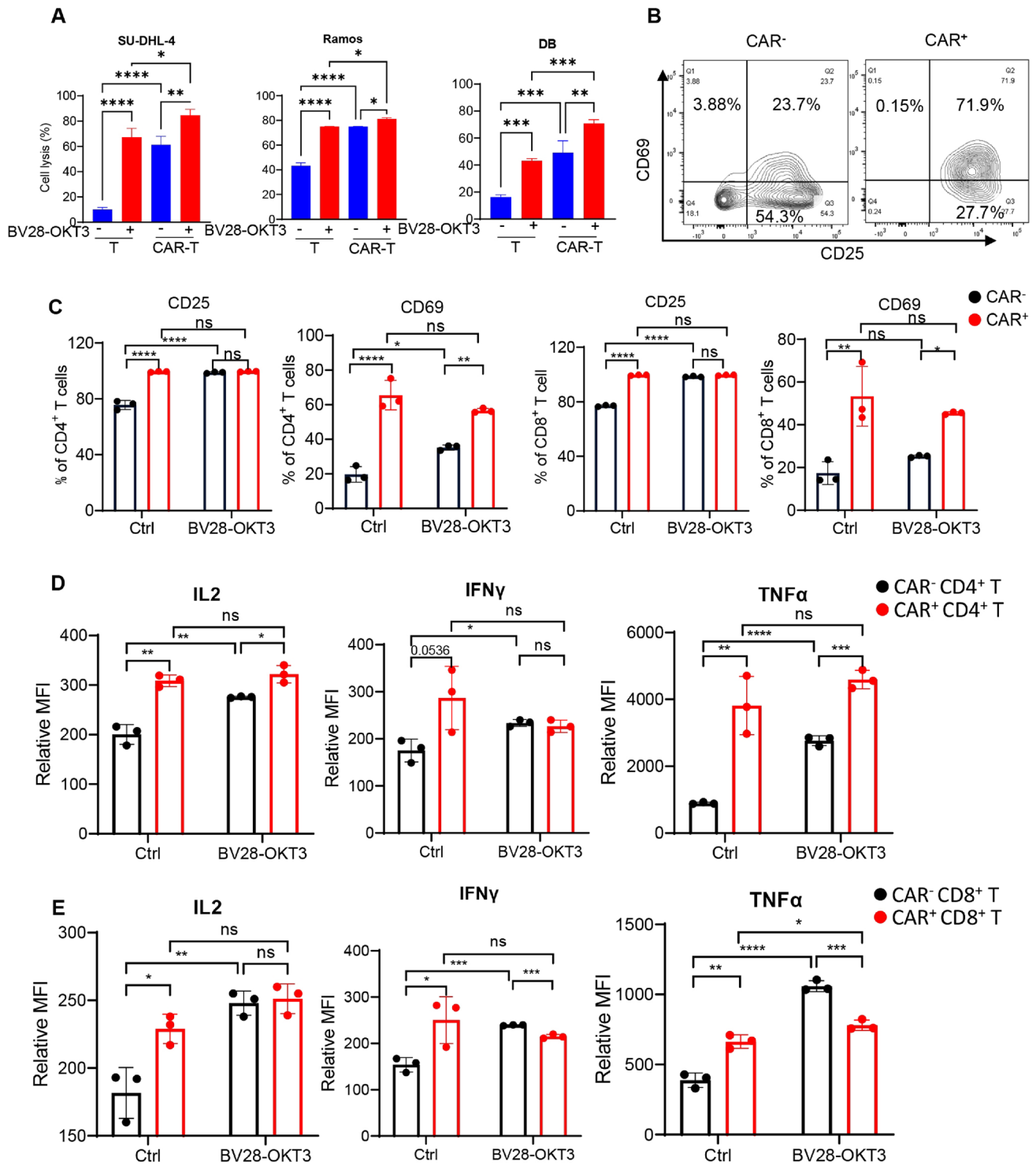


**Fig. 6** BV28-OKT3 triggers CAR-negative T-cell activation **A** T cells or CAR19-T cells were co-cultured with lymphoma cell lines at E:T as 1:1 for 24 h with or without 50 ng/mL BV28-OKT3. Cell lysis ratio was analyzed by flow cytometry; **B** CAR19-T cells were incubated with an equal number of SU-DHL-4 for 24 h, demonstrating a typical FCM graph of CD25 and CD69 expression on CAR<sup>+</sup> or CAR<sup>-</sup> T cells; **C–E** CAR19-T cells were incubated with an equal number

of SU-DHL-4 with or without 50 ng/mL BV28-OKT3 for 24 h; PBS as control. The ratio of CD69<sup>+</sup> or CD25<sup>+</sup> cells of CD4<sup>+</sup> and CD8<sup>+</sup> T cells was assessed by flow cytometry **C**. Transport protein inhibition was added 18 h after co-culturing, and the mean fluorescence intensity of IL2, IFN $\gamma$ , and TNF $\alpha$  of CD4<sup>+</sup> T cells **D** and CD8<sup>+</sup> T cells **E** was assessed by flow cytometry after 6 h

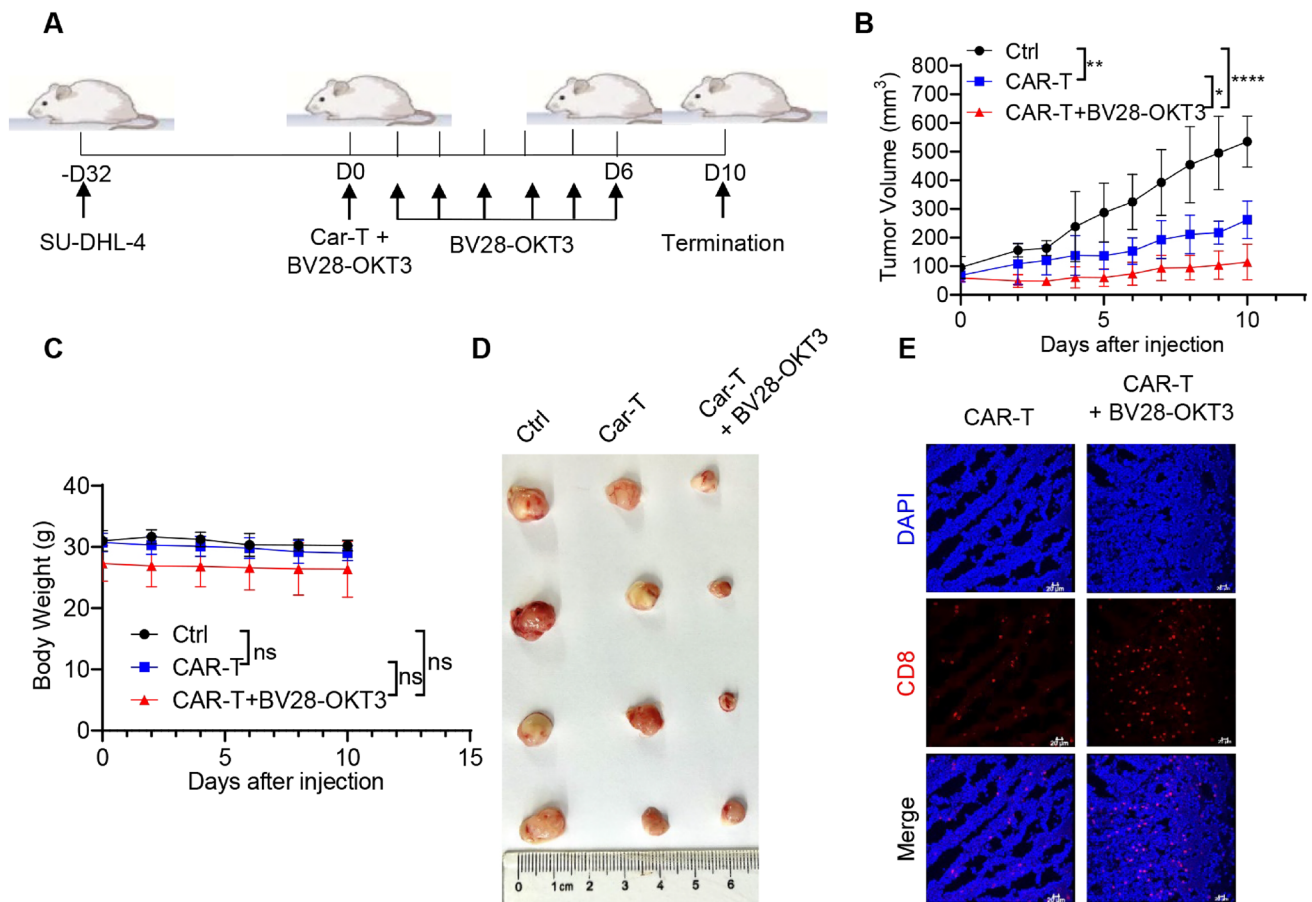


**Fig. 7** BV28-OKT3 enhances the antitumor function of CAR19-T cells in vivo **A** Schematic representation depicts the xenograft mouse model. NSG mice were subcutaneously injected with  $1 \times 10^7$  SU-DHL-4 cells. When tumors reached a volume of approximately  $100 \text{ mm}^3$ , mice were randomized into three groups and received different treatments: Control group (n=4), CAR-T group (n=4), CAR-T+BV28-OKT3 group (n=4); **B** Tumor growth curves of

all mice are presented (means  $\pm$  SD). One-way ANOVA was used for analysis at D10. \*,  $P < 0.05$ ; \*\*,  $P < 0.01$ ; \*\*\*\*,  $P < 0.0001$ ; **C** Weight change curves of all mice are shown (means  $\pm$  SD); One-way ANOVA was used for analysis at D10; **D** Images of the tumors harvested from the mice at the end of the experiment; **E** Representative tumor images obtained by confocal microscopy are shown. Blue indicates Dapi, and red indicates CD8

redirects  $\text{CD79b}^+ \text{CD19}^-$  lymphoma cells to CAR19-T cells, was developed based on the aforementioned findings.

Several studies have indicated that CAR-T cells secreting BiTEs locally have superior antitumor function than CAR-T cells alone in glioblastoma treatment, and also prevent the immune escape of CAR-T cells and recruit bystander T cells [34, 35]. This type of CAR-T therapy provided a more convenient method for clinical application and showed lower toxicity or side effects. However, the combination of BiTEs and CAR19-T cells is more flexible and the dose and usage frequency of BiTEs can be controlled. Furthermore, with the exhaustion of autocrine CAR-T cells, the amount of secreted BiTEs will decrease, while the BiTEs combined with CAR-T therapy can effectively achieve the working concentrations through exogenous supplementation.

After a single infusion, dual-targeting CAR-T therapies, such as anti-CD19 and CD22 CARs, have achieved excellent

clinical outcomes [36]. In addition, the production of dual-targeting CAR-T cells is relatively simple, using bicistronic vectors to encode both CARs and tandem CAR. However, the persistence of CAR-T cells limits the efficiency of dual-target CAR-T therapy [37]. In our study, the bispecific antibodies in combination therapy can be supplied exogenously at any time and can mobilize the endogenous T cells, which have more powerful functions than the exhausted CAR-T cells. Furthermore, combination therapy offers better flexibility in application. For example, based on the tumor antigen expression of patients, the bispecific antibodies can be combined with different CAR-T therapies instead of producing new dual-targeting CAR-T cells.

The construction of CD3-BsAbs involves various structural options [19], such as BiTEs, Diabody, knobs-in-holes, and Triomab. BiTEs comprise two different scFvs, enabling close interaction between T cells and tumor cells

because of their small size and high flexibility [22]. In addition, BiTEs have low immunogenicity because of their simple structures. From a clinical study, blinatumomab, constructed with a BiTE structure, prolonged the retention time of T cells in the bone marrow, liver, and spleen, allowing T cells to exert long-term antitumor effects [38]. BV28-OKT3, with a BiTE structure, was designed in this study, and multiple-dose administration of BV28-OKT3 preserved the antitumor function of CAR19-T cells continuously *in vivo*.

The recognition of tumor antigens by recombining TCRs on the surface of T cells drives immune-mediated tumor killing. However, T cells that specifically recognize tumor antigens are only a small fraction of tumor-infiltrating lymphocytes (TILs), while many TILs are T cells that recognize tumor-unrelated antigens (bystander or target-ignorant T cells). Reactivation of the antitumor effects of bystander T cells could help develop new therapeutic strategies for tumor immunotherapy. Bispecific antibodies, particularly BiTEs, help reinvigorate bystander T cells to attack tumors by enabling them to recognize target antigens via artificial recombinant linking molecules [39]. Our study demonstrated that BV28-OKT3 recruited CAR<sup>+</sup> and CAR<sup>-</sup> T cells into tumor tissues, reactivated the antitumor function of CAR<sup>-</sup> T cells, and recruited and reactivated the antitumor effect of donor-derived T cells. These findings suggest that BV28-OKT3 can be directly used to convert bystander (or ordinary) T cells into TILs with antitumor activity.

Tumor-associated stroma, such as fibroblasts and mesenchymal cells, form physical barriers in tumor tissue [40], and they preclude the infiltration of T cells from peripheral blood into the tumor, partially explaining why the complete response of CAR19-T cells in the treatment of lymphoma is lower than that in leukemia. Delivering immunotherapeutic molecules such as cytokines [41], immune cells [42], antibodies [43], and bacteria through intratumoral injection is a compelling approach to circumvent these barriers and is applied to a range of histological conditions and target organs, including lymphoma. In lymphoma, evidence of increased tumor infiltration by T cells was observed following the intratumoral injection of cytidine-guanosine motifs [44]. Melero et al. proposed that T-cell engagers are likely to be tested intratumorally in the future [45]. Here, BV28-OKT3 was intratumorally injected into the lymphoma of a mouse model and significantly improved the antitumor function of CAR19-T cells and promoted the infiltration of CD8<sup>+</sup> T cells into tumor tissues, thus supporting the observed *in vivo* antitumor activity. Intratumoral injection of BV28-OKT3 maintained a high local concentration and did not provoke CAR19-T cells that cause systemic side effects such as weight loss and organ injury.

Overall, an anti-CD79b/CD3 bispecific antibody, BV28-OKT3, was constructed and combined with CAR19-T

therapy to treat B-cell lymphoma. We propose a promising strategy to prevent the escape of tumor cells from CAR19-T cells owing to the loss or downregulation of the CD19 antigen and the simultaneous activation of bystander T cells to kill tumor cells. However, further studies are required to confirm their clinical efficacy.

**Supplementary Information** The online version contains supplementary material available at <https://doi.org/10.1007/s00262-023-03526-z>.

**Acknowledgements** We thank Ying An for excellent technical support.

**Author contributions** CKM, DCW and LAB: designed the study, analyzed and interpreted data, and wrote the paper; ZWW, ZH and LP performed experiments, analyzed and interpreted experimental and clinical data; YSG collected clinical samples; AT and YLT performed experiments; QK discussed results and contributed to data interpretation. All authors read and approved the final manuscript.

**Funding** This work is supported by the National Natural Science Foundation of China (NO. 81830004 to A.-B.L.; NO. 82070168 to P.L.; NO. 81800191 to K.Q.; NO. 82070158 to C.-W.D.; NO.32100747 to K.-M.C), and Translational Research Grant of NCRCH (NO. 2020ZKZC04 to A.-B.L.), and the Ministry of Science and Technology of China (NO. 2021YFA1100800 to A.-B.L.), and Shanghai Municipal Health Commission (NO. 2020CXJQ02 to A.-B.L.), and Guangxi Natural Science Foundation Program (NO. 2019GXNSFDA245031 and 2021GXNSFAA220097 to C.-W.D.), and the “Dawn” Program of Shanghai Education Commission (NO. 19SG14 to C.-W.D.), and the Program of Shanghai Academic/Technology Research Leader (NO. 21XD1422600 to C.-W.D.), and the Shanghai Sailing Program (NO.21YF1428200 to K.-M.C.).

**Data availability** The datasets generated during and/or analysed during the current study are available from the corresponding author on reasonable request.

## Declarations

**Conflict of interest** The authors declare that the research was conducted in the absence of any commercial or financial relationships that could be construed as a potential conflict of interest.

**Ethical approval** The animal study was reviewed and approved by institutional ethical review process committee.

## References

1. Wang M, Munoz J, Goy A et al (2020) KTE-X19 CAR T-cell therapy in relapsed or refractory mantle-cell lymphoma. *N Engl J Med* 382(14):1331–1342
2. Maude SL, Laetsch TW, Buechner J et al (2018) Tisagenlecleucel in children and young adults with B-cell lymphoblastic leukemia. *N Engl J Med* 378(5):439–448
3. Schuster SJ, Bishop MR, Tam CS et al (2019) Tisagenlecleucel in adult relapsed or refractory diffuse large B-cell Lymphoma. *N Engl J Med* 380(1):45–56
4. Neelapu SS, Locke FL, Bartlett NL et al (2017) Axicabtagene ciloleucel CAR T-cell therapy in refractory large B-cell lymphoma. *N Engl J Med* 377(26):2531–2544

5. Nastoupil LJ, Jain MD, Feng L et al (2020) Standard-of-care axicabtagene ciloleucel for relapsed or refractory large B-cell lymphoma: results from the US lymphoma CAR T consortium. *J Clin Oncol* 38(27):3119–3128
6. Mueller KT, Maude SL, Porter DL et al (2017) Cellular kinetics of CTL019 in relapsed/refractory B-cell acute lymphoblastic leukemia and chronic lymphocytic leukemia. *Blood* 130(21):2317–2325
7. Gardner R, Wu D, Cherian S et al (2016) Acquisition of a CD19-negative myeloid phenotype allows immune escape of MLL-rearranged B-ALL from CD19 CAR-T-cell therapy. *Blood* 127(20):2406–2410
8. Wagner J, Wickman E, Derenzo C et al (2020) CAR T cell therapy for solid tumors: bright future or dark reality? *Mol Ther* 28(11):2320–2339
9. Sotillo E, Barrett DM, Black KL et al (2015) Convergence of acquired mutations and alternative splicing of CD19 enables resistance to CART-19 immunotherapy. *Cancer Discov* 5(12):1282–1295
10. Grupp SA, Kalos M, Barrett D et al (2013) Chimeric antigen receptor-modified T cells for acute lymphoid leukemia. *N Engl J Med* 368(16):1509–1518
11. Shah NN, Johnson BD, Schneider D et al (2020) Bispecific anti-CD20, anti-CD19 CAR T cells for relapsed B cell malignancies: a phase I dose escalation and expansion trial. *Nat Med* 26(10):1569–1575
12. Braig F, Brandt A, Goebeler M et al (2017) Resistance to anti-CD19/CD3 BiTE in acute lymphoblastic leukemia may be mediated by disrupted CD19 membrane trafficking. *Blood* 129(1):100–104
13. Hamieh M, Dobrin A, Cabriolu A et al (2019) CAR T cell trogocytosis and cooperative killing regulate tumour antigen escape. *Nature* 568(7750):112–116
14. Wang LD, Clark MR (2003) B-cell antigen-receptor signalling in lymphocyte development. *Immunology* 110(4):411–420
15. D'arena G, Musto P, Cascavilla N et al (2000) Quantitative flow cytometry for the differential diagnosis of leukemic B-cell chronic lymphoproliferative disorders. *Am J Hematol* 64(4):275–281
16. Olejniczak SH, Stewart CC, Donohue K et al (2006) A quantitative exploration of surface antigen expression in common B-cell malignancies using flow cytometry. *Immunol Invest* 35(1):93–114
17. Choi Y, Diefenbach CS (2020) Polatuzumab Vedotin: a New Target for B Cell Malignancies. *Curr Hematol Malig Rep* 15(2):125–129
18. Wang J, Li C, He K et al (2022) Characterization of anti-CD79b/CD3 bispecific antibody, a potential therapy for B cell malignancies. *Cancer Immunol Immunother* 72(2):493–507
19. Wu Z, Cheung NV (2018) T cell engaging bispecific antibody (T-BsAb): from technology to therapeutics. *Pharmacol Ther* 182:161–175
20. Frankel SR, Baeuerle PA (2013) Targeting T cells to tumor cells using bispecific antibodies. *Curr Opin Chem Biol* 17(3):385–392
21. Goebeler ME, Bargou R (2016) Blinatumomab: a CD19/CD3 bispecific T cell engager (BiTE) with unique anti-tumor efficacy. *Leuk Lymphoma* 57(5):1021–1032
22. Goebeler ME, Bargou RC (2020) T cell-engaging therapies - BiTEs and beyond. *Nat Rev Clin Oncol* 17(7):418–434
23. Khalique H, Baugh R, Dyer A et al (2021) Oncolytic herpesvirus expressing PD-L1 BiTE for cancer therapy: exploiting tumor immune suppression as an opportunity for targeted immunotherapy. *J Immunother Cancer* 9(4):e001292
24. Leung WK, Ayanambakkam A, Heslop HE et al (2022) Beyond CD19 CAR-T cells in lymphoma. *Curr Opin Immunol* 74:46–52
25. Simoni Y, Becht E, Fehlings M et al (2018) Bystander CD8(+) T cells are abundant and phenotypically distinct in human tumour infiltrates. *Nature* 557(7706):575–579
26. Meier SL, Satpathy AT, Wells DK (2022) Bystander T cells in cancer immunology and therapy. *Nat Cancer* 3(2):143–155
27. Kochenderfer JN, Dudley ME, Carpenter RO et al (2013) Donor-derived CD19-targeted T cells cause regression of malignancy persisting after allogeneic hematopoietic stem cell transplantation. *Blood* 122(25):4129–4139
28. Tong C, Zhang Y, Liu Y et al (2020) Optimized tandem CD19/CD20 CAR-engineered T cells in refractory/relapsed B-cell lymphoma. *Blood* 136(14):1632–1644
29. Fry TJ, Shah NN, Orentas RJ et al (2018) CD22-targeted CAR T cells induce remission in B-ALL that is naive or resistant to CD19-targeted CAR immunotherapy. *Nat Med* 24(1):20–28
30. Kennedy GA, Tey SK, Cobcroft R et al (2002) Incidence and nature of CD20-negative relapses following rituximab therapy in aggressive B-cell non-Hodgkin's lymphoma: a retrospective review. *Br J Haematol* 119(2):412–416
31. Deeks ED (2019) Polatuzumab vedotin: first global approval. *Drugs* 79(13):1467–1475
32. Tilly H, Morschhauser F, Sehn LH et al (2021) Polatuzumab Vedotin in previously untreated diffuse large B-cell lymphoma. *N Engl J Med* 386(4):351–363
33. Ormhøj M, Scarfò I, Cabral ML et al (2019) Chimeric antigen receptor T Cells targeting CD79b show efficacy in lymphoma with or without cotargeting CD19. *Clin Cancer Res* 25(23):7046–7057
34. Choi BD, Yu X, Castano AP et al (2019) CAR-T cells secreting BiTEs circumvent antigen escape without detectable toxicity. *Nat Biotechnol* 37(9):1049–1058
35. Yin Y, Rodriguez JL, Li N et al (2022) Locally secreted BiTEs complement CAR T cells by enhancing killing of antigen heterogeneous solid tumors. *Mol Ther* 30(7):2537–2553
36. Spiegel JY, Patel S, Muffly L et al (2021) CAR T cells with dual targeting of CD19 and CD22 in adult patients with recurrent or refractory B cell malignancies: a phase I trial. *Nat Med* 27(8):1419–1431
37. Cordoba S, Onuoha S, Thomas S et al (2021) CAR T cells with dual targeting of CD19 and CD22 in pediatric and young adult patients with relapsed or refractory B cell acute lymphoblastic leukemia: a phase I trial. *Nat Med* 27(10):1797–1805
38. Bargou R, Leo E, Zugmaier G et al (2008) Tumor regression in cancer patients by very low doses of a T cell-engaging antibody. *Science* 321(5891):974–977
39. Trabolsi A, Arumov A, Schatz JH (2019) T cell-activating bispecific antibodies in cancer therapy. *J Immunol* 203(3):585–592
40. Liu Z, Zhou Z, Dang Q, Xu H, Lv J, Li H, Han X (2022) Immunosuppression in tumor immune microenvironment and its optimization from CAR-T cell therapy. *Theranostics* 12(14):6273–6290
41. Berraondo P, Sanmamed MF, Ochoa MC et al (2019) Cytokines in clinical cancer immunotherapy. *Br J Cancer* 120(1):6–15
42. Huarte E, Tirapu I, Arina A et al (2005) Intratumoural administration of dendritic cells: hostile environment and help by gene therapy. *Expert Opin Biol Ther* 5(1):7–22
43. Baniel CC, Heinze CM, Hoefges A et al (2020) In situ vaccine plus checkpoint blockade induces memory humoral response. *Front Immunol* 11:1610
44. Frank MJ, Reagan PM, Bartlett NL et al (2018) In Situ vaccination with a TLR9 agonist and local low-dose radiation induces systemic responses in untreated indolent lymphoma. *Cancer Discov* 8(10):1258–1269
45. Melero I, Castanon E, Alvarez M et al (2021) Intratumoural administration and tumour tissue targeting of cancer immunotherapies. *Nat Rev Clin Oncol* 18(9):558–576

**Publisher's Note** Springer Nature remains neutral with regard to jurisdictional claims in published maps and institutional affiliations.

Springer Nature or its licensor (e.g. a society or other partner) holds exclusive rights to this article under a publishing agreement with the

author(s) or other rightsholder(s); author self-archiving of the accepted manuscript version of this article is solely governed by the terms of such publishing agreement and applicable law.